Unusual Tuning of Mechanical Properties of Thermoplastic Elastomers Using Supramolecular Fillers

Eva Wisse,[†] L. E. Govaert,[‡] H. E. H. Meijer,[‡] and E. W. Meijer*,[†]

Laboratory of Macromolecular and Organic Chemistry, Eindhoven University of Technology, P.O. Box 513, NL-5600 MB Eindhoven, The Netherlands, and Section Materials Technology (MaTe), Eindhoven University of Technology, P.O. Box 513, NL-5600 MB, Eindhoven, The Netherlands

Received May 3, 2006; Revised Manuscript Received July 20, 2006

ABSTRACT: Supramolecular fillers were incorporated in a poly(ϵ-caprolactone)-based polyurea in a modular approach via a "perfect-fit" principle. DSC and AFM studies both support the same model in which the bis(ureido)butylene-based filler molecules are incorporated into the bis(ureido)butylene hard segment domains of the polymer via bifurcated hydrogen-bonding interactions up to 23 mol % (= 7.3 wt %) of incorporated filler. Polymer hard segment and filler form a single phase, and the soft phase remains unaffected. This resulted in stiffer materials (23 mol % of incorporated filler more than doubled the Young's modulus) without a decrease in tensile strength or elongation at break. When more than 23 mol % of filler was added to the polyurea, separate filler crystallites were observed in both AFM and DSC. A drop in Young's modulus was now observed, followed by an increase upon adding even more filler. In this second regime, a decrease in tensile strength and elongation at break was observed, revealing similar behavior to reinforcing thermoplastic elastomers with the more common micrometer-sized reinforcement fillers.

Introduction

Reinforcement fillers are used extensively to improve stiffness of thermoplastic elastomers. However, because of the rigidity of most fillers, the polymer becomes also more brittle. The increase in stiffness depends mainly on size, shape, and interfacial adhesion between the polymer and the surface of the filler.[1] In general, smaller sized fillers give better mechanical properties, higher Young's modulus, and less reduced tensile strength and elongation at break. The smallest fillers have the largest surface area, resulting in an improved filler−matrix interaction.[2] To improve interfacial adhesion, chemical or physical bonding between filler and matrix has been introduced. Dubois et al.[3] applied the polymerization filling technique to improve the interfacial adhesion between filler and polymer by in-situ polymerization on the filler surface. Chantaratcharoen et al.[4] used chemical modification of reinforcing fibers to improve filler−matrix adhesion. They showed improved tensile strength and elongation at break as compared to nontreated fillers. However, compared to the unfilled polymers, tensile strength and elongation at break still decreased when filler was added.

An alternative approach to stiffen thermoplastic elastomers is to increase the hard block to soft block ratio (HB/SB) in the polymer chain. According to Wegner,[5] the logarithm of the Young's modulus of segmented copolymers follows a linear relationship with the volume fraction of crystallinity. He showed this relation for copolymers with a constant PTMO (poly(tetramethylene oxide)) soft segment (M_n = 1000 g/mol) and PBT (poly(butylene terephthalate)) hard segments of varying lengths. The same relation is valid for poly(ϵ-caprolactone)-based polyurethanes where the HB/SB ratio was altered by varying soft segment length.[6] Also here an increase in stiffness was accompanied by a decrease in both tensile strength and strain at break.

From the literature cited above it becomes clear that two general methods to increase the stiffness of a thermoplastic elastomer are used. First, reinforcement fillers can be mixed with the thermoplastic elastomer. This will result in a second, separate filler hard phase besides the hard and soft phase already present in the polymer chains of the segmented copolymer. Second, the ratio of hard and soft segments can be varied in the polymer chains. This can be achieved by varying either the soft or the hard block length. Both methods can increase the stiffness of thermoplastic elastomers, but simultaneously tensile strength and strain at break are reduced. The first approach needs significantly higher amounts of additional hard segments to increase the stiffness to the same extent as compared to the second method. Here, we demonstrate the unusual properties of a supramolecular filler that is only incorporated in the hard segments of a well-defined thermoplastic elastomer via supramolecular interactions, an approach recently introduced by us.[7] In this way a combination of the two described methods is realized: filler is mixed with the thermoplastic elastomer, but filler and polymer hard segments now form a single hard phase. The block copoly(ester)urea ($PCLU_4U$) used consists of a poly(ϵ-caprolactone) (PCL, M_n = 1446 g/mol) soft segment and a well-defined hard segment consisting of two urea groups separated by a fixed spacer length (Figure 1, $M_{bisurea}$ = 172.2 g/mol; 10.6 wt % of hard segments). The hard segments of these polymers self-assemble into supramolecular ribbons and form reversible cross-links. In our modular approach, guest molecules bearing a bis(ureido)butylene moiety are incorporated in the supramolecular ribbons of the thermoplastic elastomer via a "perfect-fit" principle (Figure 1).[8] By mixing supramolecular filler with $PCLU_4U$, we circumvent the problem of packing characteristics, size, and shape of the more traditional micrometer sized fillers by using a molecular sized filler. Since filler and hard segments of the polymer form a single hard phase, we expect excellent interfacial adhesion and no interference with the soft phase. A maximum of 23 mol % could be incorporated before the filler gradually started to phase separate from the

[†] Laboratory of Macromolecular and Organic Chemistry.
[‡] Section Materials Technology (MaTe).
* Corresponding author. E-mail: E.W.Meijer@tue.nl.

10.1021/ma060986i CCC: $33.50
Published on Web 09/21/2006

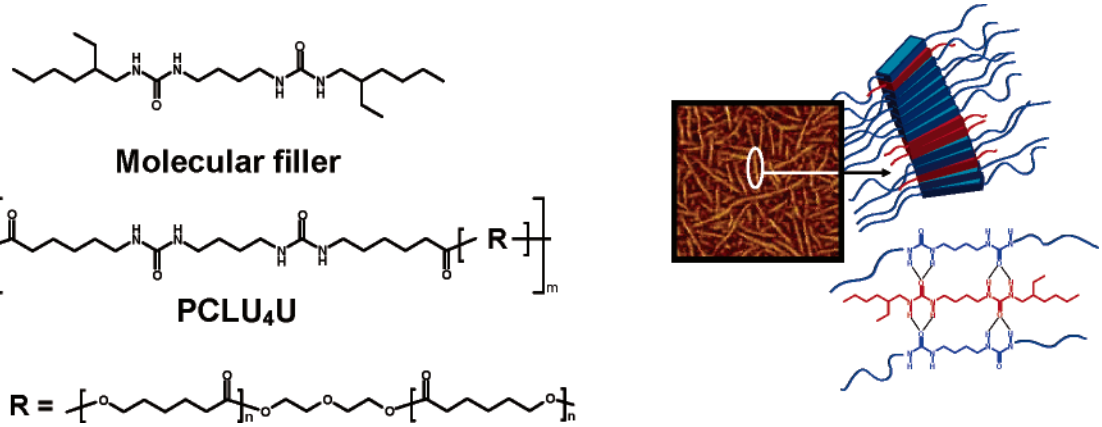

Figure 1. Proposed modular approach: the supramolecular filler (red) is incorporated into the $PCLU_4U$ hard domains (blue) via bifurcated hydrogen bonds.

polymer hard segments. The Young's modulus was increased over 100% without a decrease in tensile strength or strain at break.

Experimental Section

Materials and General Synthetic Procedures. All reagents and solvents were purchased from commercial sources and were used without further purification. Chloroform was dried over 4 Å molsieves (Merck). All reactions were carried out under a dry argon atmosphere. Infrared spectra were measured on a Perkin-Elmer Spectrum One FT-IR spectrometer with a Universal ATR sampling accessory. ^{1}H NMR and ^{13}C NMR spectra were recorded on a Varian Gemini (300 MHz for ^{1}H NMR, 75 MHz for ^{13}C NMR) or a Varian Mercury (400 MHz for ^{1}H NMR, 100 MHz for ^{13}C NMR) spectrometer at 298 K. Matrix-assisted laser desorption/ionization mass time-of-flight spectra (Maldi-TOF) were obtained using α-cyano-4-hydroxycinnamic acid as the matrix on a PerSeptive Biosystems Voyager-DE PRO spectrometer.

Synthesis of 1-(2-Ethylhexyl)-3-{4-[3-(2-ethylhexyl)ureido]-butyl}urea. The supramolecular filler was synthesized by dissolving 2-ethyl-1-hexylamine (3.69 g, 28.6 mmol) in 60 mL of dry $CHCl_3$. A solution of diisocyanatobutane (0.9 mL, 7.14 mmol) in 10 mL of dry $CHCl_3$ was added by drops. The reaction was allowed to stir until no isocyanate functionalities were observed with infrared spectroscopy. All solvent was evaporated, and the reaction mixture was redissolved in THF and subsequently precipitated in 0.1 M hydrochloric acid. The product was washed with 0.1 M hydrochloric acid and neutral water before it was dried in a vacuum overnight. The product was dissolved in $CHCl_3$ and dried with Na_2SO_4. The product was obtained as a white powder in a 99.4% yield. Melting point = 117 °C. FT-IR: 3330, 2958, 2925, 2860, 1624, 1564, 1480, 1459, 1379, 1258, 1234, 1142, 1066, 774 cm^{-1}. ^{1}H NMR ($CDCl_3$): δ 4.99 + 4.77 (t, 4H, N*H*), 3.20 (m, 4H, NHC*H*$_2$(CH$_2$)$_3$), 3.08 (m, 4H, NHC*H*$_2$CH), 1.51 (m, 4H, NHCH$_2$C*H*$_2$), 1.40 (m, 2H, C*H*), 1.34−1.26 (m, 16H, CH$_3$C*H*$_2$C*H*$_2$C*H*$_2$), 0.88 (m, 12H, C*H*$_3$) ppm. ^{13}C NMR ($CDCl_3$): 159.7 (C=O), 43.2 (*C*H), 40.0 (NH*C*H$_2$), 31.0 (CH$_3$*C*H$_2$CH), 29.0 (CH$_2$*C*H$_2$CH), 28.1 (NHCH$_2$*C*H$_2$), 24.1 (CH$_3$CH$_2$*C*H$_2$), 23.1 (CH$_3$*C*H$_2$CH$_2$), 14.1 and 10.9 (*C*H$_3$) ppm. MALDI−TOF: calculated mass: 398.63 g/mol, observed mass: 399.56 g/mol.

Synthesis of $PCLU_4U$. Poly(ϵ-caprolactone) (M_n = 1250, 20 g, 16 mmol), *N*-carbobenzoxy-6-aminohexanoic acid (9.3 g, 36.8 mmol), 4-(dimethylamino)pyridinium 4-toluenesulfonate (DPTS)[12] (1.18 g, 4 mmol), and *N*,*N*′-dicyclohexylcarbodiimide (DCC) (9.9 g, 48 mmol) were dissolved in 300 mL of dry $CHCl_3$, and the reaction was allowed to stir for 48 h. The reaction mixture was filtrated and solvent was evaporated. The remaining solid material was dissolved in 100 mL of $CHCl_3$ and precipitated in heptane to obtain PCL(C5-NH-Z)$_2$, a white powder in a 90% yield. A solution of PCL(C5-NH-Z)$_2$ (10 g, 5.8 mmol) in 250 mL of EtOAc/MeOH (v/v 4:1) and 1 g of 10% Pd supported on activated carbon was subjected to hydrogenation under a H_2 blanket at room temperature overnight. After filtration over Celite, the product was isolated by precipitation in hexane, resulting in PCL(C5-NH$_2$)$_2$, a white powder in a 95% yield. PCL(C5-NH$_2$)$_2$ (10 g, 6.8 mmol) was dissolved in 150 mL of dry $CHCl_3$. A solution of 850 μL of 1,4-diisocyanatobutane in 5 mL of $CHCl_3$ was slowly added by drops until the methylene protons next to the amine were no longer visible in ^{1}H NMR. $PCLU_4U$ was isolated in a 90% yield by precipitation in hexane. FT-IR: ν = 3323, 2940, 2864, 1728, 1616, 1576 cm^{-1}. ^{1}H NMR ($CDCl_3$): δ = 4.24 (t, 4H), 4.04 (t, 2(2*n*)H), 3.70 (t, 4H), 3.14 (b, 8H), 2.32 (t, 2(2*n* + 2)H), 1.66 (m, 2(4*n* + 2)H), 1.49 (m, 8H), 1.39 (m, 2(2*n* + 2)H) ppm. ^{13}C NMR ($CDCl_3$): δ = 173.5, 159.0, 69.0, 64.1, 63.2, 40.0, 39.8, 34.0, 30.0, 27.6, 26.3, 28.3, 25.4, 24.5 ppm.

Preparation of Polymer Films. All samples were prepared by dissolving the right amounts of supramolecular filler and $PCLU_4U$ together in chloroform. Films for DSC were prepared by drop-casting these solutions (100 mg in 3 mL) in Teflon dishes of 45 × 25 × 5 mm. The dishes were covered with a spoutless beaker to allow the solvent to evaporate slowly. Further drying in a vacuum at 40 °C overnight resulted in solvent free films. Approximately 3−10 mg of each film was used for DSC measurements. Films for tensile testing were prepared by drop-casting these solutions (1.5 g in 15 mL) in Teflon dishes of 105 × 45 × 5 mm. The dishes were covered with a spoutless beaker to allow the solvent to slowly evaporate. After thermally annealing at 80 °C for 4 h tensile bars (according to ASTM D 1708-96 dimensions) were punched from the resulting films. Samples for AFM were prepared by dissolving 1 mg of the films that were prepared for DSC measurements in 1 mL of chloroform and were subsequently drop-cast on glass coverslips that were cleaned by sonicating in acetone for 15 min and subsequently dried under vacuum at 40 °C for a few hours.

Differential Scanning Calorimetry. DSC measurements were performed on a Perkin-Elmer differential scanning calorimeter Pyris 1 with Pyris 1 DSC autosampler and Perkin-Elmer CCA7 cooling element under a nitrogen atmosphere. Melting and crystallization temperatures were determined in the second heating run at a heating/cooling rate of 10 °C min^{-1} and glass transition temperatures at a heating rate of 40 °C min^{-1}.

Atomic Force Microscopy. AFM images were recorded at 37 °C in air using a Digital Instrument Multimode Nanoscope IV operating in the tapping regime mode using silicon cantilever tips (PPP-NCH-50, 204−497 kHz, 10−130 N/m). Scanner 6007JVH was used with scan rates between 0.5 and 1 Hz. All images are subjected to a first-order plane-fitting procedure to compensate for sample tilt.

Tensile Testing. Tensile properties were measured according to ASTM D 1708-96 in air at 37 °C. Thickness of the samples was always very close to 0.3 mm. Grip to grip separation was <22 mm due to limited dimensions of the used climate chamber. Testing was conducted in a Zwick Z100 universal tensile tester

Scheme 1. Synthetic Route to $PCLU_4U$

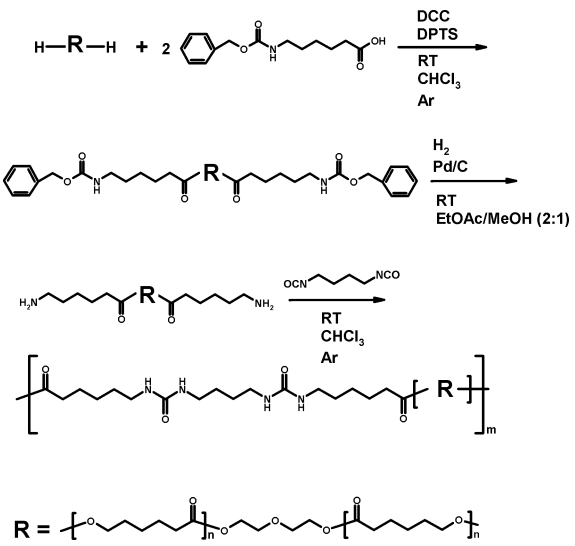

equipped with a 2.5 kN or 100 N load cell. A Noske-Kaeser TEE_180/1N2_(80)_X climate chamber was used around the test specimens. The crosshead speed was 20 mm/min. Between 4 and 6 samples were evaluated for each polymer/filler ratio to determine *E*, yield stress, and yield strain. Because of slipping of some samples from the clamps at higher elongations, the tensile strength, strain at break, and toughness could be determined from 3 to 5 samples per polymer/filler ratio. Exceptions: for 3.8 mol %: $n = 1$ (though elongations of 2790 and 3500% and corresponding tensile strengths of 17.3 and 17.7 MPa were reached without failure, further elongation could not be reached due to the limiting dimensions of the climate chamber) and for 50 mol %: $n = 2$. Because of the shape of the stress−strain curves, yield stresses and strains were determined as the intersection point of the two tangents to the initial and final parts of the load elongation curves at the yield point.[9] An indicative Young's modulus was determined by calculating the slope at 0% strain.

Results

Synthesis of Supramolecular Filler and $PCLU_4U$. The molecular filler was prepared by adding a solution of 1,4-diisocyanatobutane in chloroform dropwise to a solution of 4 equiv of 2-ethylhexylamine in chloroform. The product was isolated in high yields by precipitation from THF in 0.1 M hydrochloric acid. In differential scanning calorimetry (DSC) a melting peak was observed at 117 °C. The product was further characterized by NMR, IR, and mass spectrometry. The synthesis of $PCLU_4U$ was not straightforward since functionalizing the PCL prepolymer with amine end groups easily results in amide formation. To circumvent this problem, PCL-diol (M_n = 1250) was reacted with benzyl-protected aminohexanoic acid in a DCC coupling using DPTS as a catalyst. The resulting product was stable in time. Directly after deprotection of the amine, exactly 1 equiv of 1,4-diisocyanatobutane was added by drops to obtain maximum chain extension (Scheme 1). In this way, no amidation was observed, and the characterization of the polymer by NMR, IR, and GPC fully confirmed the structure assigned. GPC showed a molecular weight of M_n = 56 kg/mol (M_w = 109 kg/mol, PD = 1.9). $PCLU_4U$ shows a glass transition temperature at −56.5 °C, a melting peak at 17 °C of the poly(ϵ-caprolactone) soft block, and a melting peak at 107 °C of the bis(ureido)butylene hard segments in DSC. The synthesis of various batches leads to small but insignificant differences in glass and melting transitions for the different $PCLU_4U$ samples. For all measurements reported in this paper the data of a single batch are used.

Thermal Properties. The clear difference in melting temperatures for the bis(ureido)butylene hard segments of the polymer and the supramolecular filler can be employed to study the thermal properties of $PCLU_4U$ containing different amounts of supramolecular filler. The supramolecular based composites were prepared by dissolving both compounds in various ratios in chloroform and subsequent solution casting of these solutions. In DSC, measured between 50 and 140 °C, the melting peaks in the second heating runs were evaluated. The results are plotted in Figure 2A,B. The bis(ureido)butylene units of the pure polymer showed a melting peak at 107 °C. Upon adding more and more filler to $PCLU_4U$, we observed one melting transition that was decreasing a few degrees in melting temperature upon adding the supramolecular filler. Simultaneously, the melting enthalpy (ΔH_m) increased (Figure 3). However, when 28.6 mol % of filler was present in the polymer, a second melting transition appeared (Figure 2B), accompanied by a drop in ΔH_m. Continuing to incorporate more filler, the first melting transition remained around the same temperature of ∼102 °C, while the melting temperature of the newly observed melting transition gradually shifted toward the melting temperature of the pure filler. The melting enthalpy (ΔH_m) of this second melting peak increased when more filler was added. It was not always possible to determine the melting enthalpies of the two observed melting transitions separately due to some peak overlap. However, the total ΔH_m increased upon adding more filler above 28 mol %. Finally, the glass transition temperature of the PCL soft block was measured and showed only a slight decrease of 3 °C over the range of compositions (Figure 2C).

Surface Morphology. Hard segment morphologies of thermoplastic elastomers were investigated using atomic force microscopy (AFM).[10] Especially phase images obtained with this imaging technique provided useful information and proved to be reasonably representative for bulk morphologies.[11] In phase images the hard phase of the polymer appears brighter than the soft phase. AFM topography and phase images were recorded in tapping mode in air at 37 °C; from DSC it is known that the PCL soft block is completely amorphous at this temperature. In this way the semicrystallinity of PCL was not interfering in imaging the hard segment morphology. Phase as well as height images of $PCLU_4U$ showed a typical fiberlike morphology of hard segments embedded in a soft matrix. The diameter of the observed fibers was measured to be 5−6 nm in all cases. When 1 mol % of filler was added, the surface morphology looked very much alike. When more and more filler was added, up to 23 mol %, always similar surface morphologies were observed with similar fiber diameters. From 3.8 up to 23 mol % filler, small white features of ∼1 nm thickness were observed in the phase images (Figure 4). Phase images showed them to be relatively hard with more white features at higher filler content. These features, however, were not always evenly distributed over the surface (for an example, see Supporting Information Figure 1). When more than 23 mol % filler was added to $PCLU_4U$ films, and even already on some locations of the 23 mol % sample, white features started to cluster and formed bigger aggregates covering the whole surface. The white features were proposed to be the crystals of filler. As a result, no fiberlike morphology was observed anymore (see Supporting Information Figure 2).

Mechanical Properties. Tensile tests were performed in air at 37 °C to eliminate the influence of the semicrystallinity of PCL, as was done with the AFM study. The results are listed in Table 1 and plotted in Figure 5, derived from engineering stress−strain curves. Figure 6 is based on the true stress−

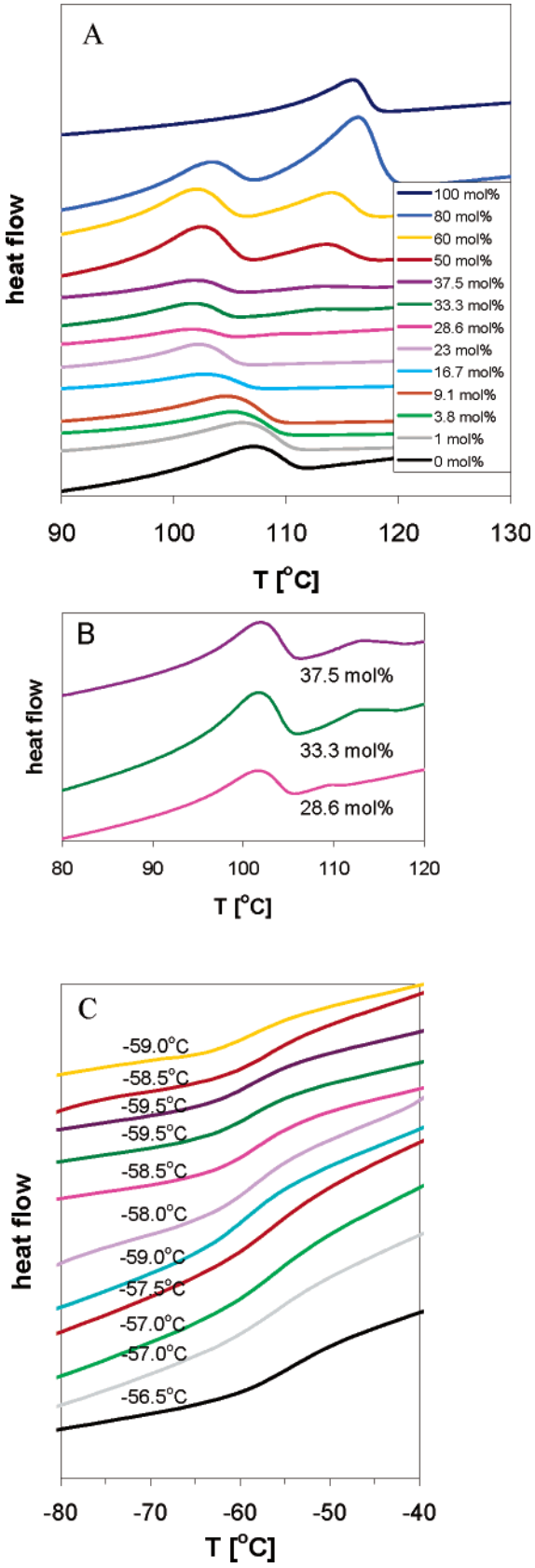

Figure 2. DSC curves (Endo Up) of various amounts of filler in $PCLU_4U$ for (A) melting temperatures, (B) zoom of melting temperatures of three samples, and (C) glass transition temperatures.

elongation curves. With increasing amount of molecular filler in $PCLU_4U$, the Young's modulus increased up to 29 MPa at 28.6 mol %, more than double the value of the pristine $PCLU_4U$

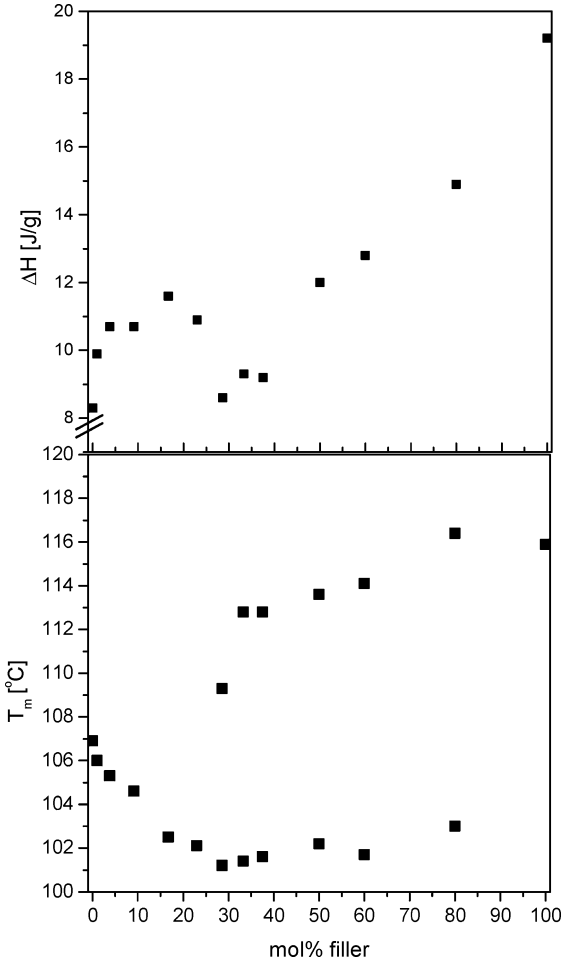

Figure 3. Melting temperatures (bottom) as a function of supramolecular filler added to $PCLU_4U$ and ΔH_m (top), derived from DSC curves in Figure 2A.

(Figure 6A). The maximum was expected to lie between 23 (7.3 wt %) and 28.6 mol % (9.5 wt %) according to the DSC measurements. When more than 28.6 mol % was added, a drop in Young's modulus was observed, followed by a gradual increase upon adding even more of the supramolecular filler. The yield stress remained constant up to 16.7 mol %, with a small decrease at 23 and 28.6 mol % and remained significantly lower afterward (Figure 6B). Tensile strength and strain at break were surprisingly not decreasing with increasing amount of incorporated filler up to 28.6 mol %. The slightly lower value at 16.7 mol % of filler, accompanied by a higher standard deviation, was attributed to the use of two polymer films for the determination of the tensile properties. One film apparently was of slightly lower quality, resulting in three samples that reached elongations at break around 2400% (true tensile strength ~325 MPa). A second film was of better quality, resulting in two samples breaking over 3200% of elongation (true tensile strength ~510 MPa). When more than 28.6 mol % of molecular filler was added, a decreasing trend for both tensile strength and elongation at break was observed (Figure 6C,D). In Figure 6C,D the error bars around the transition going from the first to the second regime are significantly larger as compared to the other error bars. This and the decreasing values of the yield stress at 23 and 28.6 mol % of filler indicate there is not a sudden transition from the first to the second regime, but rather one that is more gradual in nature.

The logarithm of the Young's modulus follows a linear relationship with the volume fraction of crystallinity in the

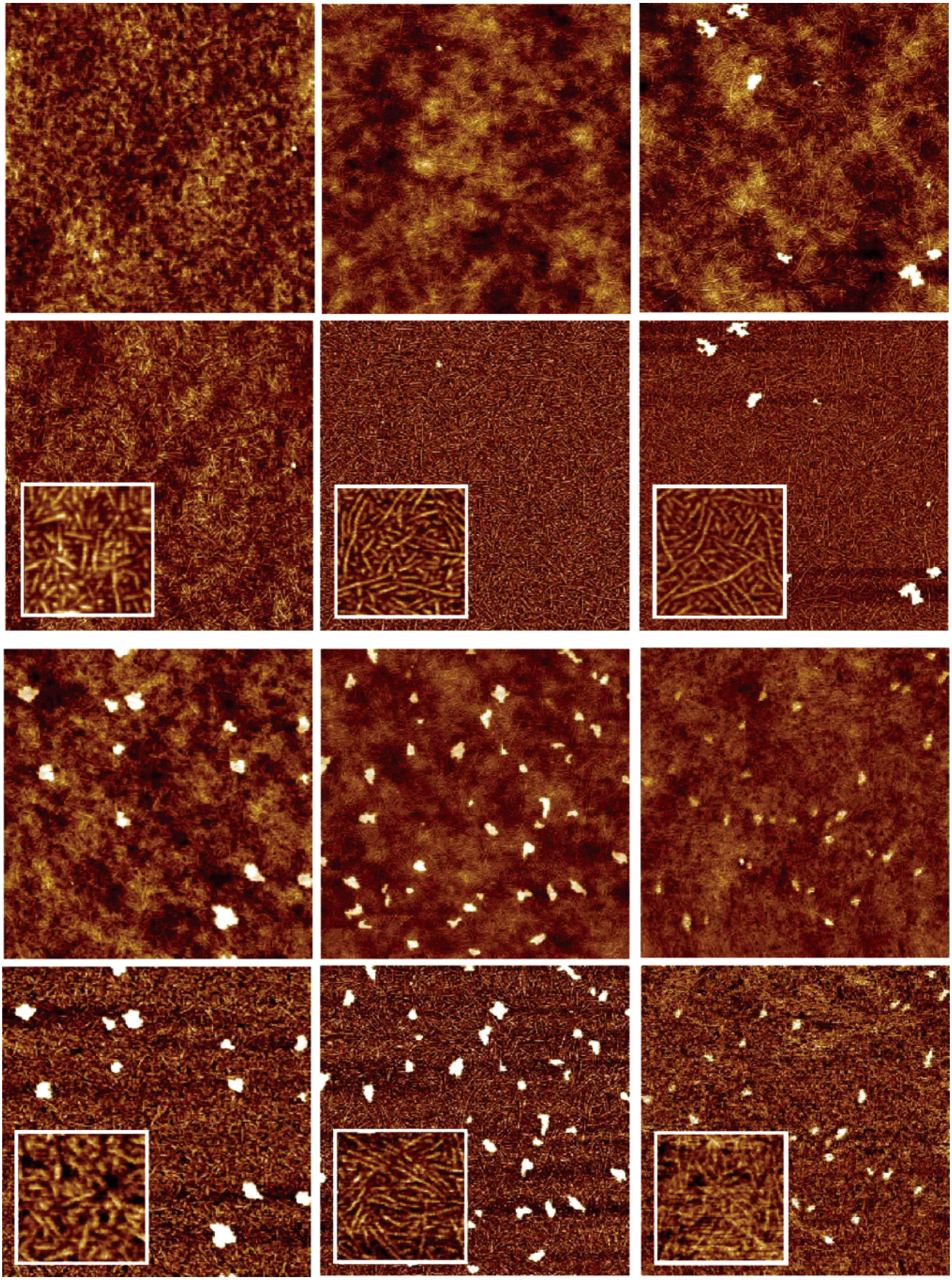

Figure 4. AFM topography (top) and phase (bottom) images at 1 μm scan sizes (insets: 150 nm) of PCLU$_4$U containing increasing amounts of molecular filler: (A) 0, (B) 1, (C) 3.8, (D) 9.1, (E) 16.7, and (F) 23 mol %. *Z* ranges are 3, 5, 5, 5, 8, and 10 nm in (A)−(F), respectively. $\Delta\varphi$ is 10°, 10°, 12°, 6°, 12°, and 5° for (A)−(F), respectively. Data obtained in tapping mode in air at 37 °C.

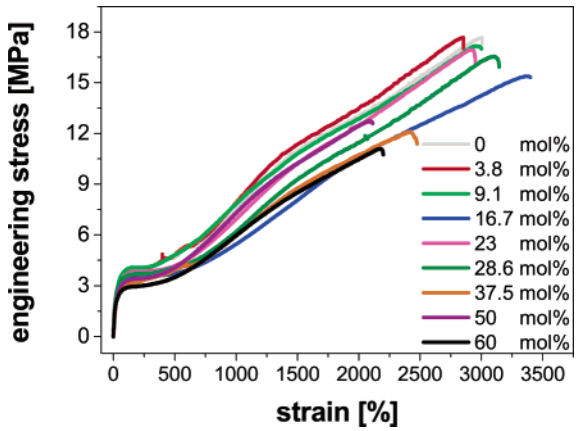

Figure 5. Representative engineering stress−elongation curves for $PCLU_4U$ with various amounts of incorporated supramolecular filler.

regime up to 28.6 mol % of filler. Since there is no crystallinity in the pCL phase at 37 °C, this corresponds to the calculated weight fraction of bisurea hard segments ($M_{bisurea}$ = 172.2 g/mol). We compared this relation for our data with the data of poly(ϵ-caprolactone)-based polyurethanes where the HB/SB ratio was altered by varying soft segment length.[6] The slope for the former is 3 times higher (13.8) than the slope of the latter (14.5) (see Supporting Information Figure 3).

Table 1. Mechanical Properties of $PCLU_4U$ Containing Increasing Amounts of Filler; Data Derived from Engineering $\sigma-\epsilon$ Curves

amount of filler in $PCLU_4$4 [mol %]	E [MPa]	σ_{yield} [MPa]	ϵ_{yield} [%]	σ_{max} [MPa]	ϵ_{break} [%]
0	11.8 ± 1.5	3.8 ± 0.1	35.9 ± 4.0	17.9 ± 1.0	3000 ± 60
3.8	11.6 ± 1.7	3.7 ± 0.2	34.8 ± 3.5	17.0[a]	3020[a]
9.1	13.0 ± 3.3	3.8 ± 0.3	28.3 ± 3.5	17.0 ± 0.6	2920 ± 160
16.7	19.8 ± 1.5	3.8 ± 0.4	20.8 ± 2.7	14.2 ± 0.8	2710 ± 600
23	23.1 ± 3.9	3.9 ± 0.3	17.0 ± 3.1	17.8 ± 2.0	2910 ± 350
28.6	28.7 ± 3.8	3.7 ± 0.1	14.4 ± 0.5	15.1 ± 2.2	2920 ± 300
37.5	21.6 ± 1.3	3.2 ± 0.1	16.7 ± 2.3	13.3 ± 2.4	2710 ± 220
50	24.9 ± 2.1	3.2 ± 0.1	17.1 ± 0.6	12.7 ± 0.1[b]	2130 ± 2[b]
60	25.5 ± 3.5	2.8 ± 0.1	13.1 ± 1.3	10.9 ± 0.6	2100 ± 180

[a] $n = 1$. [b] $n = 2$.

Discussion

In an unusual way, we have tuned the mechanical properties of our $PCLU_4U$ thermoplastic elastomer by incorporating supramolecular fillers via a modular approach. By mixing only 7.3 wt % (23 mol %) of our supramolecular filler in $PCLU_4U$, it is possible to increase the Young's modulus from 12 to 29 MPa. Concurrently, the yield stress, tensile strength, and strain at break are not influenced by the filler. To our knowledge, similar results have never been reported with other fillers or by changing the hard block−soft block (HB/SB) ratio. According

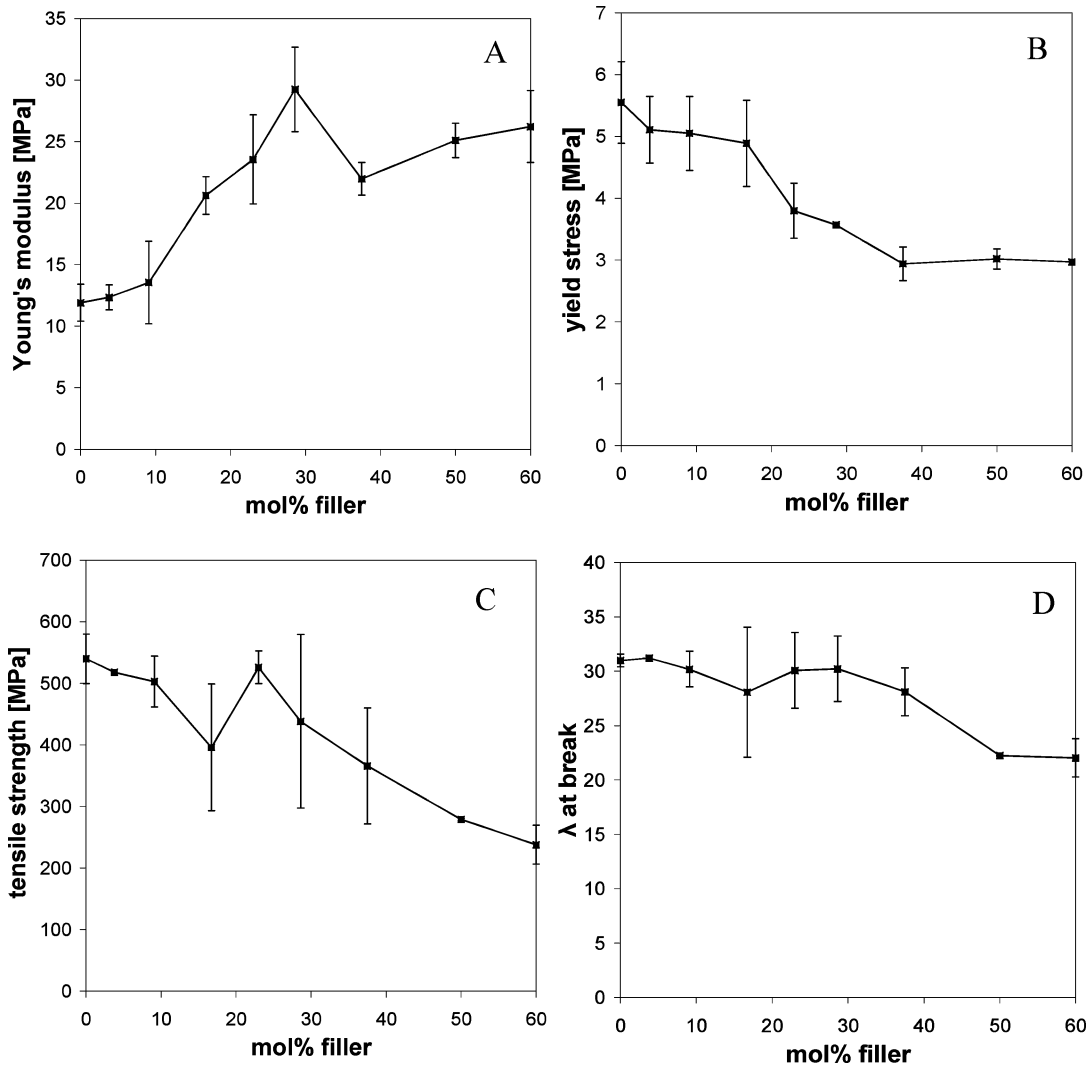

Figure 6. Young's modulus (A), yield stress (B), tensile strength (C), and λ at break (D) of $PCLU_4U$ films containing increasing amounts of filler. Data derived from true $\sigma-\lambda$ curves.

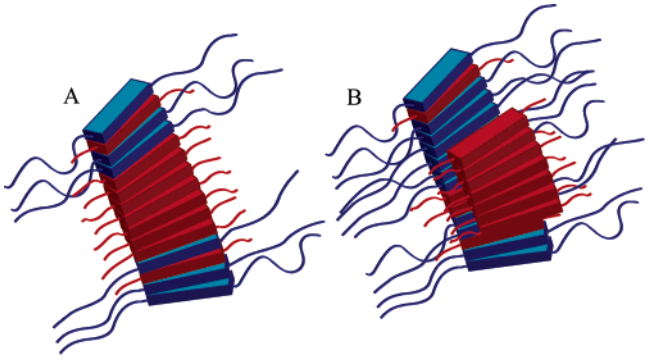

Figure 7. Schematic representation for two possible molecular interpretations of the regime above 23 mol % of filler.

to Wegner,[5] a linear relationship between log(*E*/MPa) and the HB content was found. With a slope of 13.8, the effect is significantly higher than by increasing the HB/SB ratio in the traditional way by changing the lengths of both segments. In the latter, the data of Heijkants et al.[6] yield a slope of 4.5 by varying the soft block length in the covalent polymer chain. This difference and the notion that only in our case the other mechanical properties are not affected by increasing the *E* modulus prompt us to propose a molecular picture of our modular approach using the DSC and AFM data.

The pristine polymer, consisting of a polydisperse PCL soft block and monodisperse small bisurea hard block, forms well-known morphologies: nanofibers embedded into a soft matrix.[7,10] The nanofibers with a T_m of 107 °C have a very high aspect ratio with a diameter of 5−6 nm. Since these fibers have monodisperse diameters, they are expected to have a cylindrical morphology, most probably consisting of a few bisurea stacks aligned together. By adding the supramolecular filler, we identify at first glance two regimes in the phase diagram. At concentrations of filler below 28 mol %, intimate mixing between filler and hard segment of the polymer is observed. The morphology as studied by AFM hardly changes (the small filler crystallites are assumed to be a surface phenomenon, only, since in this regime no evidence for a separate hard phase is found in DSC), while the T_m and T_g are only slightly shifted (less than 5 °C).

For concentrations of 28 mol % and higher, both DSC and AFM show the presence of crystallites of only the filler as a second hard phase. DSC in this regime shows a separate melting transition for the filler. Where DSC measurements are representative for the bulk sample, AFM only shows the morphology of the surface, and therefore quantitative data are hard to discern from these AFM measurements. From the phase diagram in Figure 2 a sudden transition from the first regime to the second regime could be assumed between 23 and 28.6 mol % of filler. However, in AFM measurements at 23 mol % the surface morphology was very inhomogeneous, with sometimes morphologies as shown in Figure 4, but also the onset of clustering of the small filler crystallites to larger aggregates was observed (data not shown). Together with the more deviating ΔH_m data between approximately 23 and 37.5 mol % filler from Figure 3, this gives rise to the idea of another regime: a less-defined transition regime when going from a single phase of filler and polymer hard segments to a situation where also a separate filler hard phase is present. As a result, also the homogeneity of the sample will be less. This assumption grows stronger when looking at the mechanical properties.

In the first regime, the Young's modulus increases over 100% without a decrease in tensile strength or strain at break. All the filler is present in the hard segment stacks of the polymer, leaving the polymer soft matrix unaffected (Figure 1). The significantly larger error bars around the transition from the first to the second regime in the tensile strength and elongation at break together with the decreasing values of the yield stress at 23 and 28.6 mol % once more indicate the existence of a transition regime. In the second regime, significant amounts of separate filler crystallites are present. The Young's modulus showed a slower increase and tensile strength and strain at break are decreasing. The mechanical behavior in this second regime seems similar to the incorporation of more common micrometer sized fillers. When we think of possible molecular understanding in this regime, we could think of two options: large domains of filler still present in the same bisurea stacks, large enough to be visible by DSC (Figure 7A), or a physically separate filler hard phase (Figure 7B).

Conclusions

A new way to increase stiffness in thermoplastic elastomers is introduced. In this method a supramolecular filler is introduced in the bis(ureido)butylene stacks of a segmented copoly(ester)-urea. DSC, AFM, and mechanical analysis all support the same model in which the molecular filler is completely implemented in the bis(ureido)butylene stacks of the polymer up to approximately 23 mol % (7.3 wt %) via supramolecular interactions. In this way we are able to increase the Young's modulus from 12 to 29 MPa without a reduction in tensile strength or strain at break. Compared to using the more common micrometer-sized reinforcement fillers, the same amount of filler results in a much higher increase in Young's modulus in our case.[1a,2a] Furthermore, the fact that molecular filler and the hard segments of our thermoplastic elastomer form a single phase provides excellent interfacial adhesion and is responsible for an unaffected soft matrix. A 3 times higher slope of the straight line in a log(*E*/MPa) vs hard segment content plot shows that, also compared to the second method, as described in the Introduction, our approach results in a larger increase in stiffness. In our system the increase of the hard phase in the HB/SB ratio is not in the direction of the covalent polymer chains, but in a direction perpendicular to the covalent chain. In this way the covalent polymer chains are unaffected altogether. Most probably it is this property that causes the remarkable mechanical behavior.

Acknowledgment. The authors thank A. J. H. Spiering for synthesizing $PCLU_4U$ and R. P. Sijbesma for useful discussions. Financial support from the Netherlands Technology Foundation (STW) and the Chemical Council of the Dutch National Science Foundation (CW-NWO) is gratefully acknowledged.

Supporting Information Available: AFM topography and phase images of $PCLU_4U$ containing 9.1 mol % (Figure S1) and 28.6 mol % (Figure S2) of filler; plot (Figure S3) of relation between log(*E*) and hard segment content. This material is available free of charge via the Internet at http://pubs.acs.org.

References and Notes

(1) (a) Hiljanen-Vainio, M.; Heino, M.; Seppälä, J. V. *Polymer* **1998**, *39*, 865−872. (b) Katz, H. S.; Milewski, J. V. *Handbook of Fillers and Reinforcements for Plastics*; van Nostrand Reinhold Co.: London, 1978; p 652. (c) Funabashi, M.; Hirose, S.; Hatakeyama, T.; Hatakeyama, H. *Macromol. Symp.* **2003**, *197*, 231−241.

(2) (a) Ismail, H.; Salmah, Bakar, A. A. *J. Reinf. Plast. Compos.* **2005**, *24*, 147−159. (b) Samoilov, V. M.; Ostronov, B. G. *Inorg. Mater.* **2004**, *40*, 359−363. (c) Juhasz, J. A.; Best, S. M.; Brooks, R.; Kawashita, M.; Miyata, N.; Kokubo, T.; Nakamura, T.; Bonfield, W. *Biomaterials* **2004**, *25*, 949−955. (d) Busigin, C.; Lahtinen, R.; Martinez, G. M.; Thomas, G.; Woodhams, R. T. *Polym. Eng. Sci.* **1984**, *24*, 169−174.

(3) Dubois, P.; Alexandre, M.; Jérôme, R. *Macromol. Symp.* **2003**, *194*, 13−26.
(4) (a) Chantaratcharoen, A.; Sirisinha, C.; Amornsakchai, T.; Bualek-Limcharoen, S.; Meesiri, W. *J. Appl. Polym. Sci.* **1999**, *74*, 2414−2422. (b) Saikrasun, S.; Amornsakchai, T.; Sirisinha, C.; Meesiri, W.; Bualek- Limcharoen, S. *Polymer* **1999**, *40*, 6437−6442.
(5) Wegner, G. In Legge, N. R.; Holden, G.; Schroeder, H. E. *Thermoplastic Elastomers: A Comprehensive Review*; Carl Hansser Verslag: New York, 1987; p 250.
(6) Heijkants, R. G. J. C.; van Calck, R. V.; van Tienen, T. G.; de Groot, J. H.; Buma, P.; Pennings, A. J.; Veth, R. P. H.; Schouten, A. J. *Biomaterials* **2005**, *26*, 4219−4228.
(7) (a) Versteegen, R. M.; Sijbesma, R. P.; Meijer, E. W. *Macromolecules* **2005**, *38*, 3176−3184. (b) Versteegen, R. M.; Kleppinger, R.; Sijbesma, R. P.; Meijer, E. W. *Macromolecules* **2006**, *39*, 772−783.
(8) Koevoets, R. A.; Versteegen, R. M.; Kooijman, H.; Spek, A. L.; Sijbesma, R. P.; Meijer, E. W. *J. Am. Chem. Soc.* **2005**, *127*, 2999−3003.
(9) Ward, I. M.; Sweeney, J. *An Introduction to the Mechanical Properties of Solid Polymers*, 2nd ed.; John Wiley & Sons: Weinheim, 2004.
(10) (a) Shet, J. P.; Wilkes, G. L.; Fornof, A. R.; Long, T. E.; Yilgor, I.; *Macromolecules* **2005**, *38*, 5681−5685. (b) Garrett, J. T.; Siedlecki, C. A.; Runt, J. *Macromolecules* **2001**, *34*, 7066−7070. (c) Revenko, I.; Tang, Y.; Santerre J. P. *Surf. Sci.* **2001**, *491*, 346−354.
(11) (a) Pfau, A.; Janke, A.; Heckmann, W. *Surf. Interface Anal.* **1999**, *27*, 410−417. (b) Wu, W.; Huang, J.; Jia, S.; Kowalewski, T.; Matyjaszewski, K. *Langmuir* **2005**, *21*, 9721−9727.
(12) Moore, J. S.; Stupp, S. I. *Macromolecules* **1990**, *23*, 65−70.

MA060986I